

ULTRAFAST ELECTRON DIFFRACTION SYSTEM AT THE NSLS SDL*

Y. Hidaka[#], C. C. Kao, J. B. Murphy, S. Pjerov, B. Podobedov, H. Qian, S. Seletskiy, Y. Shen, X. J. Wang, X. Yang, NSLS, Brookhaven National Laboratory, Upton, NY 11973, U.S.A.

Abstract

Ultrafast electron diffraction (UED) is a promising technique that allows us to observe a molecular structure transition on the time scale on the order of femtoseconds. Present state-of-the-art UED systems utilize sub-relativistic electron bunches as the probing beam. With such low energy, however, the number of electrons in the bunch must be significantly decreased for a short bunch length (~100 fs) due to the space charge effect. This limits the detection capability of such keV UED devices. To overcome this issue, a UED system using an MeV electron beam has been proposed, and designed at Source Development Laboratory (SDL) in National Synchrotron Light Source (NSLS). The detailed system design and the major hardware components are presented in this paper as well as the numerical analysis of this system using the particle tracking code, GPT, from the photocathode to the detector.

INTRODUCTION

Ultrafast science is growing rapidly around the world and includes a broad range of scientific disciplines such as biology, chemistry, and materials science [1-3]. One of the promising tools used in this field, ultrafast electron diffraction (UED), has been continuously developed as a complementary technology to X-ray free electron lasers (X-FELs). The UED has several advantages over X-FELs in terms of its compactness, 6 orders of magnitude larger cross section, and less damaging ability to the samples being probed. Currently, the most advanced UED systems utilize DC electron guns as a source of probing electron beams [4,5]. However, the kinetic energy achievable by these DC guns is limited to typically on the order of keV. At this low energy level, the space charge effect is significant and prohibits the generation of short electron bunches. The bunch length can be shortened to ~100 fs only if the number of electrons in the bunch is significantly decreased, but at the cost of much weaker

diffraction signals. This makes it impossible to conduct single-shot diffraction experiments with these keV UED systems. To overcome this issue, a UED system with a photocathode RF gun that generates an MeV electron beam has been proposed [6,7], and designed at Source Development Laboratory (SDL) in National Synchrotron Light Source (NSLS). Encouraged by the studies reported earlier, employing the same concept [8-10], we expect our system should prove to be a substantial upgrade to the UED technology. This paper presents the status on the progress of research and development of our UED system.

HARDWARES

The design layout of the whole UED assembly at the NSLS SDL is shown in Fig. 1. All the major components, such as a klystron, an RF gun, a solenoid, and a deflecting cavity, shown in Fig. 2, have been acquired, being tested for performance, and ready to be assembled and commissioned soon.

The electron source is a slightly modified version of the standard 2.856-GHz, 1.6-cell BNL-type RF gun that has been developed mainly for free electron lasers (FELs) and

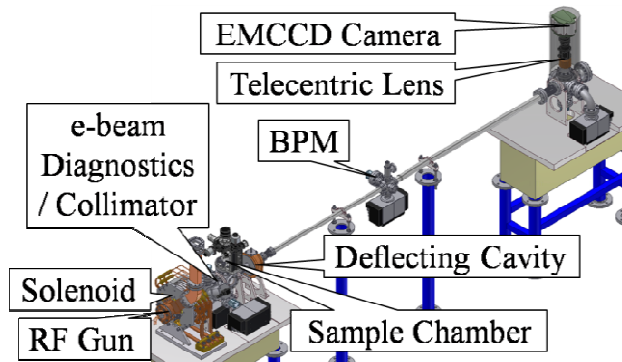


Figure 1: Schematic of the whole UED system.

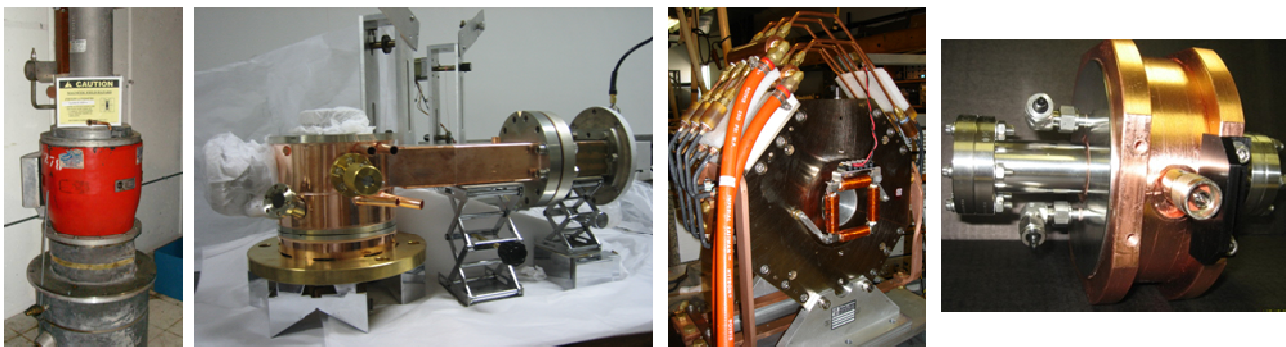


Figure 2: Photographs of the S-band klystron, photocathode RF gun, solenoid, and RF deflecting cavity.

*Work supported by US DOE contract No. DE-AC02-98CH1-886.

[#]yhidaka@bnl.gov

other applications in the last few decades. The UED RF gun uses a shorter solenoid than the standard one, since the UED system requires much less electron beam energy than applications like FELs. Another advantage of a shorter solenoid is the expected reduction of the quadrupole component in the solenoid field. The solenoid must have azimuthal openings so that the cooling water can circulate through the solenoid. The solenoid has four azimuthally symmetrical openings to minimize asymmetry introduced by the required openings, but inevitably acquires a small quadrupole component. Thus, it is best to have the shortest length possible for the solenoid to minimize the distortion in the diffraction patterns due to the quadrupole field effect.

The titanium sapphire laser system generates two pulses, one of which is the pump pulse to initiate the reaction of the sample, and the other is the UV pulse to hit the photocathode and generate electrons.

Right after the solenoid, there is a steering magnet that was accurately calibrated; it will be used for misalignment correction, as well as for measuring the electron energy accurately with less than 1-2% error. An e-beam diagnostic chamber with a tungsten beam collimator is located after the trim magnet. Inside this chamber, a phosphor screen followed by a 45-degree copper mirror serves as a destructive absolute energy and charge measurement tool when used in conjunction with the trim magnet. Then lies a sample chamber, which has a sample holder located at about 60 cm downstream from the photocathode surface. Another diagnostic equipment placed right after the sample chamber is a deflecting cavity (Haimson Research Corp.). This cavity should allow us to measure the electron bunch length with the time resolution up to 20 fs for the beam with an emittance smaller than 0.1 mm-mrad.

After a ~3.5-m drift section with another beam position monitor in the middle, there is a detector chamber that houses a high-efficiency phosphor screen and a 45-degree copper mirror. The light emitted by the screen is collected by a telecentric lens followed by an electron multiplying charge coupled device (EMCCD) camera.

The unique feature of this screen-mirror system, as shown in Fig. 3, is that both the screen and the mirror have holes at the centers. Since most of the electrons are not scattered by the sample, and pass near the center of the screen, the light intensity near the center will be very high without the holes. This will cause two problems: 1) The excessively intense light will reflect off the chamber wall and most likely contaminate the diffraction pattern as an additional background noise; 2) The intense hot spot at the center can damage the EMCCD camera, if the gain is increased high enough to detect weak diffraction rings. However, the hole in the screen solves these issues so that the full dynamic range of the camera can be utilized. The mirror with a center hole works as a Faraday cup to directly measure how much charge is actually scattered, excluding the non-scattered electrons.

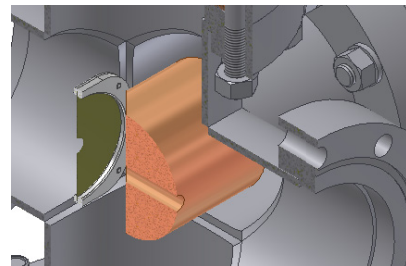


Figure 3: Screen-mirror system with center holes in the detector chamber.

The EMCCD camera (Andor iXon DV887) was chosen primarily because it has single photon detection capability with 16-bit digitization. Together with this highly sensitive camera, the low f-number and minimal image distortion of the telecentric lens (Schneider Xenoplan Telecentric 1:5) ensures that the best possible diffraction patterns can be obtained with our UED system.

SIMULATIONS

The UED system described above has been analyzed by using a commercially available particle tracking code, GPT, from start to end [11]. Simulations have been performed in three steps. First, electrons are injected into the simulation volume from the gun cathode, and the particles are tracked with the precise electromagnetic field data of the RF gun cavity obtained from SUPERFISH [12] and the solenoid magnetostatic field data obtained from RADIA [13]. In the second step, scattering by an ideal polycrystalline aluminum thin foil is simulated. A custom GPT scattering element has been written based on the scattering algorithm, the details of which are outlined in [14]. The second step imports all the particle information from the first step, and exports the new particle information with the added angular kicks calculated by the scattering element. In the third step, these scattered particles are imported and tracked until they hit the detector screen ~4 m downstream from the sample location. In all the steps above, all Coulomb interactions are accounted for so that both the space

Table 1: Design Parameters

UV Laser	
Transversely uniform, hard-edge radius	0.2 mm
Longitudinally Gaussian, pulse width (rms)	300 fs
RF Gun	
Gradient	45.1 MV/m
Electron pulse launch phase	15°
Solenoid Strength	
	0.1 T
Electron Bunch at the Sample	
Bunch charge	48 fC
Kinetic energy	2 MeV
Relative energy spread (rms)	9.5×10^{-4}
Pulse width (rms)	179 fs
Divergence (rms)	59 μ rad
Spot size (rms)	200 μ m

charge and stochastic effects are included in the simulations.

Figure 4(a) shows a part of a simulated diffraction pattern. The parameters assumed in this simulation are listed in Table 1. This simulation also assumed an initial normalized thermal emittance of 35.6 nm, estimated from the formula in [15] for the parameters listed in Table 1. The blue curve in Fig. 4(b) represents the histogram of Fig. 4(a) against the radial position from the beam axis. The red curve in Fig. 4(b) shows the histogram in the case of zero initial thermal emittance.

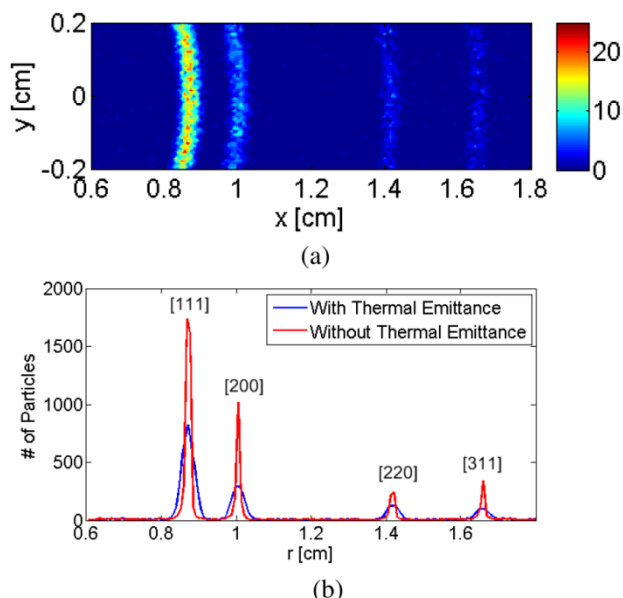


Figure 4: (a) A part of the simulated diffraction pattern with non-zero thermal emittance, represented as a pseudo-color intensity plot. The unit of the colorbar values is the number of electrons in each cell (80 μm by 80 μm). (b) The histogram of (a) against the radial coordinate (blue curve). The ideal case of zero thermal emittance is also plotted as the red curve for comparison.

The severe degradation in sharpness of the diffraction peaks due to the thermal emittance is evident from the two curves. Nonetheless, all the rings are still well separated. This is largely due to the relatively low energy we selected, compared to the energy used in the previous studies [8,9]. The angular position θ_{hkl} of a diffraction ring from a polycrystalline sample is determined by the Bragg's Law:

$$\theta_{hkl} = \frac{\lambda}{a_0} \sqrt{h^2 + k^2 + l^2} \quad (1)$$

where a_0 is the structure constant of the sample, and λ is the de Broglie wavelength, and the Miller indices h , k , l specify the orientation of the crystal plane. Since λ is inversely proportional to the relativistic factor γ , the lower the energy is, the wider the separation between the rings becomes. Another reason for the clear separation of the rings is because the solenoid strength was adjusted such that the electron beam hits the sample at a converging

angle [16]. With the beam hitting a sample at the beam waist or, even worse, at a diverging angle, the diffraction image gets substantially blurred.

Further numerical optimization will be performed to search parameters with better diffraction pattern characteristics, and understand the beam physics that leads to those desirable results.

SUMMARY

The design of the MeV UED system at the NSLS SDL has been discussed in detail. All the major hardware components have been obtained and are ready to be assembled. The whole system should be commissioned by the end of 2009. The diffraction patterns predicted by simulations are promising, even with a realistic initial thermal emittance and the space charge calculation included from start to end.

ACKNOWLEDGMENTS

We would like to thank R. K. Li for helpful discussions on simulations, and G. Rakowsky and D. Harder for help on the solenoid magnetic field simulation and measurements.

REFERENCES

- [1] A. Robinson *et al.*, "Science and Technology of Future Light Sources," ANL-08/39, BNL-81895-2008, LBNL-1090E-2009, SLAC-R-917 (December, 2008).
- [2] G. Mourou and S. Williamson, *Appl. Phys. Lett.* **41**, 44 (1982).
- [3] A. H. Zewail, *Annu. Rev. Phys. Chem.* **57**, 65 (2006).
- [4] D. Shorokhov and A. H. Zewail, *Phys. Chem. Chem. Phys.* **10**, 2879 (2008).
- [5] S. Nie, X. Wang, H. Park, R. Clinite and J. Cao, *Phys. Rev. Lett.* **96**, 025901 (2006).
- [6] X. J. Wang, Z. Wu and H. Ihee, PAC03, 420 (2003).
- [7] X. J. Wang, D. Xiang, T. K. Kim and H. Ihee, *J. Korean Phys. Soc.* **48**, 390 (2006).
- [8] J. B. Hastings *et al.*, *Appl. Phys. Lett.* **89** 184109 (2006).
- [9] P. Musumecchi *et al.*, *Ultramicroscopy* **108**, 1450 (2008).
- [10] R. K. Li, C. X. Tang, Y. Du, W. Huan, Q. Du, J. Shi, L. Yan and X. J. Wang, submitted for publication.
- [11] <http://www.pulsar.nl/gpt>
- [12] POISSON/SUPERFISH Group of Codes, LA-UR-87-115, Los Alamos, NM (1987).
- [13] <http://www.esrf.eu/Accelerators/Groups/InsertionDevices/Software/Radia>
- [14] F. M. Rudakov *et al.*, *AIP Conf. Proc.* **845**, 1287 (2006).
- [15] J. E. Clendenin *et al.*, *Nucl. Instr. and Meth. A* **455**, 198 (2000).
- [16] A. Gahlmann, S. T. Park and A. H. Zewail, *Phys. Chem. Chem. Phys.* **10**, 2894 (2008).